J. Fluid Mech. (1997), *vol.* 350, *pp.* 271–293. Printed in the United Kingdom

Linear stability of rotating convection in an imposed shear flow

By PAUL MATTHEWS AND STEPHEN COX

Department of Theoretical Mechanics, University of Nottingham, University Park, Nottingham NG7 2RD, UK

(Received 9 July 1996 and in revised form 14 April 1997)

In many geophysical and astrophysical contexts, thermal convection is influenced by both rotation and an underlying shear flow. The linear theory for thermal convection is presented, with attention restricted to a layer of fluid rotating about a horizontal axis, and plane Couette flow driven by differential motion of the horizontal boundaries.

The eigenvalue problem to determine the critical Rayleigh number is solved numerically assuming rigid, fixed-temperature boundaries. The preferred orientation of the convection rolls is found, for different orientations of the rotation vector with respect to the shear flow. For moderate rates of shear and rotation, the preferred roll orientation depends only on their ratio, the Rossby number.

It is well known that rotation alone acts to favour rolls aligned with the rotation vector, and to suppress rolls of other orientations. Similarly, in a shear flow, rolls parallel to the shear flow are preferred. However, it is found that when the rotation vector and shear flow are parallel, the two effects lead counter-intuitively (as in other, analogous convection problems) to a preference for oblique rolls, and a critical Rayleigh number below that for Rayleigh–Bénard convection.

When the boundaries are poorly conducting, the eigenvalue problem is solved analytically by means of an asymptotic expansion in the aspect ratio of the rolls. The behaviour of the stability problem is found to be qualitatively similar to that for fixed-temperature boundaries.

Fully nonlinear numerical simulations of the convection are also carried out. These are generally consistent with the linear stability theory, showing convection in the form of rolls near the onset of motion, with the appropriate orientation. More complicated states are found further from critical.

1. Introduction

Thermal convection in a horizontal layer of fluid has served for a century as the archetypal model for many buoyancy-driven geophysical and astrophysical flows. For large-scale motions, however, the rotation of the frame of reference in which the fluid motion takes place must be considered when the Rossby number is small. Furthermore, atmospheric and oceanographic convection will often take place in a background wind or current, which leads to the consideration of thermal convection in a shear flow.

Although in applications of interest the parameters may be far from the linear regime, it is important to proceed systematically and to understand the linear and weakly nonlinear behaviour of rotating convection in a shear flow before embarking

on highly nonlinear computations. We therefore solve in this paper the linear stability problem for a rotating, unstably stratified shear flow in a horizontal fluid layer. We restrict our work to the case in which the rotation vector lies in the horizontal plane, corresponding to equatorial motions. This restriction reduces the number of external parameters of the problem and allows some analytical progress to be made that is difficult to achieve for the more general case. In addition, it allows a simple Couette flow to be considered – if the rotation vector has a vertical component then the equilibrium shear flow has the structure of an Ekman spiral. We allow the angle ψ between the rotation axis and the shear flow to be arbitrary. The special cases $\psi = 0$ and $\psi = \pm\pi/2$ have been analysed by others (Hathaway, Toomre & Gilman 1980; Kropp & Busse 1991; Busse & Kropp 1992).

In the absence of a shear flow and rotation, in an infinite horizontal layer of fluid, there is no preferred orientation of convection rolls. This rotational degeneracy is broken by the imposition of a shear flow or by rotation about an axis that has some horizontal component. Our objective in this paper is to determine the preferred orientation of convection rolls for different values of the magnitude and direction of the shear flow and rotation vector.

It is not our intention to review the vast literature on thermal convection. In work directed at elucidating the role of rotation in geophysical and astrophysical contexts, most attention has been given to convection at a latitude of 90°, where the rotation vector is vertical. A tilted rotation vector, corresponding to a more general choice of latitude, has also received some attention (Chandrasekhar 1961; Busse 1982).

Analytical, numerical and experimental results on the stability of an unstably stratified non-rotating shear flow were reviewed by Kelly (1994). In a moderate shear flow, in the x-direction, say, the most unstable mode is a system of longitudinal rolls, whose axes are parallel to the x-axis. The stability problem for such rolls is unaffected by the shear flow, while oblique rolls have a larger critical Rayleigh number. The most heavily damped rolls are transverse to the shear flow. If the Reynolds number is large enough and the shear flow is of Poiseuille or mixed Couette–Poiseuille type, a hydrodynamic instability of the shear flow itself can interact with the thermal instability (Fujimura & Kelly 1988, 1995; Mohamad & Viskanta 1989). In this case, the marginal curve may have a double minimum, one corresponding to each mode of instability. However, pure Couette flow is linearly stable for all Reynolds numbers, and there is no evidence of coupling between thermal and hydrodynamic instabilities according to linear theory; the marginal curves of Deardorff (1965) and Gallagher & Mercer (1965), for example, have a single minimum. There may, however, be significant coupling when the fully nonlinear equations are considered, as Clever & Busse (1992) have demonstrated: for example, three-dimensional convection may occur at values of the Rayleigh number far below critical.

The combined effects of rotation and imposed shear have been analysed in special cases by Kropp & Busse (1991) and Busse & Kropp (1992), for thermal convection between differentially heated coaxial cylinders that rotate about their common axis. By assuming a narrow gap between the cylinders, they reduced the problem to an equivalent problem in a plane layer. Kropp & Busse (1991) took the special case in which the angular velocity vector is at right-angles to the direction of the imposed shear flow, and considered not only the linear stability of the conduction state, but also weakly nonlinear convection. They identified longitudinal and transverse rolls (with axes aligned parallel and perpendicular to the direction of the shear flow, respectively) as being of particular significance, but discovered that other, oblique,

rolls could be preferred in certain parameter ranges. Busse & Kropp (1992) examined a system similar to our plane layer but with the shear flow and rotation vector aligned. A counter-intuitive, but nonetheless correct, result of their analysis is that although the rotation and shear flow would individually impose a preference for longitudinal rolls, in combination they select oblique rolls.

Hathaway *et al.* (1980) considered the linear stability of a rotating fluid layer subject to a thermal wind (shear flow) perpendicular to the rotation vector. Their work was motivated by planetary flows, and they considered the stability problem at a variety of latitudes. They found that with a thermal wind in the east–west direction and the horizontal component of the rotation vector in the north–south direction the most unstable mode of convection takes the form of rolls with axes aligned either north–south (transverse) or east–west (longitudinal), depending on the parameters of the system; there is a critical value of the thermal wind at which a changeover takes place.

Hathaway & Somerville (1986) described numerical simulations of convection in a rotating fluid layer. A shear flow was maintained by differential motion of the boundaries, with a fictitious force introduced to fix the shear flow to be plane Couette flow rather than an Ekman spiral. A series of simulations at $Ra = 10^4$ was performed, with or without imposed shear and rotation, and at a variety of latitudes (but not at zero latitude). The simulations were of rather a short duration, and it is not clear that all transients had died away.

Our work begins in §2 by setting out the linearized equations of motion for disturbances to an unstably stratified Couette flow in a rotating frame. We then formulate the eigenvalue problem from which we calculate the critical Rayleigh number for the onset of instability. Some special cases of the problem can be treated analytically; these are described in §3 and compared with previous results. More generally, a numerical solution is necessary, and these follow in §4. The concept of a winding number is introduced to clarify the way in which the orientation of the critical rolls varies as a function of the orientation of the rotation axis relative to the shear flow. In this section the limits of large rotation rate and strong shear are treated, for the case of alignment between the rotation axis and the shear flow. Some direct numerical simulations of the full nonlinear governing equations are reported in §5, and these confirm the predictions of the linearized theory for the preferred orientation of the convection rolls. By considering the case when the boundaries are poor conductors of heat (§6), it is possible to solve the linear stability problem exactly as an asymptotic expansion in the aspect ratio of the rolls. In this way some features of the stability problem can be treated in more detail. Finally, §7 draws together our results and indicates directions for future research.

2. Governing equations

We consider convection in a layer of incompressible, Boussinesq fluid with kinematic viscosity ν and thermal diffusivity κ. Motion of the fluid is described relative to a Cartesian coordinate system (x^*, y^*, z^*) that rotates with angular velocity $\boldsymbol{\Omega}^*$. The fluid is confined between rigid boundaries at $z^* = \pm d/2$, and these boundaries move with prescribed speeds $\pm U_0/2$ in the x^*-direction. Provided the rotation vector $\boldsymbol{\Omega}^*$ lies in the (x^*, y^*)-plane, the motion of the boundaries induces a Couette shear flow $\boldsymbol{U}_0^* = (U_0 z/d, 0, 0)$ in the fluid layer. We suppose also that the fluid layer is heated from below, maintaining a temperature gradient across the layer, with the temperature given by $T^* = T_0 - \Delta T z^*/d$. This combination of velocity and temperature fields (together

with a corresponding pressure field) is an equilibrium solution of the Navier–Stokes equation, and forms the basic state whose stability we examine below. Dimensionless variables are introduced by scaling with the depth of the layer d, the thermal timescale d^2/κ and the temperature difference across the layer ΔT. The asterisks that denote dimensional variables are dropped for their dimensionless counterparts.

The linearized Navier–Stokes and heat equations governing perturbations to the basic state are

$$\frac{1}{\sigma}\frac{\partial \boldsymbol{u}}{\partial t} + Re\, z\frac{\partial \boldsymbol{u}}{\partial x} + wRe\,\hat{\boldsymbol{x}} - 2\boldsymbol{u}\times\boldsymbol{\Omega} = -\nabla p + Ra\,\theta\hat{\boldsymbol{z}} + \nabla^2\boldsymbol{u}, \tag{2.1}$$

$$\frac{\partial\theta}{\partial t} - w + \sigma Re\, z\frac{\partial\theta}{\partial x} = \nabla^2\theta, \tag{2.2}$$

together with the continuity equation $\nabla\cdot\boldsymbol{u} = 0$. Here $\boldsymbol{u} = (u, v, w)$ is the fluid perturbation velocity, θ is the temperature perturbation from equilibrium and $p = d^2p^*/(\rho\kappa\nu)$ is the perturbation pressure. The dimensionless parameters appearing are the Prandtl number $\sigma = \nu/\kappa$, the Reynolds number of the shear flow $Re = U_0 d/\nu$, the dimensionless rotation vector $\boldsymbol{\Omega} = \boldsymbol{\Omega}^* d^2/\nu$ and the Rayleigh number $Ra = g\gamma\Delta T d^3/(\nu\kappa)$, where g is the acceleration due to gravity and γ is the coefficient of cubical expansion. With no loss of generality we take $Re \geqslant 0$. We denote the basis vectors of the coordinate system by $\hat{\boldsymbol{x}}$, $\hat{\boldsymbol{y}}$ and $\hat{\boldsymbol{z}}$.

We follow the standard treatment (Chandrasekhar 1961) of these linearized equations, by taking $\hat{\boldsymbol{z}}\cdot\nabla\times$(2.1) and $\hat{\boldsymbol{z}}\cdot\nabla\times\nabla\times$(2.1) and seeking normal modes proportional to $\exp\{ikx + ily + \lambda t\}$. Then the following replacements can be made:

$$\frac{\partial}{\partial t} = \lambda, \qquad \frac{\partial}{\partial x} = ik, \qquad \frac{\partial}{\partial y} = il. \tag{2.3}$$

There results an eigenvalue problem for the growth rate λ consisting of equations for the components of vertical velocity w and vertical vorticity ω, and the temperature perturbation θ:

$$(Re\, l + 2\Omega_1 k + 2\Omega_2 l)w = (\mathrm{D}^2 - k^2 - l^2 - Re\, zik - \lambda/\sigma)i\omega, \tag{2.4}$$

$$(2\Omega_1 k + 2\Omega_2 l)i\omega = -Ra(k^2 + l^2)\theta + (\mathrm{D}^2 - k^2 - l^2 - Re\, zik - \lambda/\sigma)(\mathrm{D}^2 - k^2 - l^2)w, \tag{2.5}$$

$$-w = (\mathrm{D}^2 - k^2 - l^2 - \sigma Re\, zik - \lambda)\theta, \tag{2.6}$$

where $\mathrm{D} = \mathrm{d}/\mathrm{d}z$. In each equation the exponential factor has been cancelled, and the remaining unknowns are functions of z alone. We impose the conditions of no slip ($\boldsymbol{u} = \boldsymbol{0}$) and constant temperature ($\theta = 0$) at the horizontal boundaries $z = \pm 1/2$.

In general the eigenvalues λ are not restricted to be real, except for some particular parameter ranges (see §3.1): λ may be complex if σ is either small or large, as found by Kropp & Busse (1991). However, in all cases we have studied, the mode of maximum growth rate (maximized over k and l) does have λ real. In this case we seek neutral modes by setting $\lambda = 0$.

It is convenient to introduce two geometrical angles (see figure 1). The angle between the rotation vector and the positive x-direction (the direction of the imposed shear flow) is denoted by ψ, so $\boldsymbol{\Omega} = (\Omega\cos\psi, \Omega\sin\psi, 0)$ with $\Omega \geqslant 0$. The wave vector can also be given an amplitude and a phase, so $k = K\cos\phi$ and $l = K\sin\phi$ with $K \geqslant 0$. Longitudinal rolls thus correspond to $\phi = \pm\pi/2$, transverse rolls to $\phi = 0$, and oblique rolls to $\phi \neq 0, \pm\pi/2$. With this notation, the eigenvalue problem for Ra

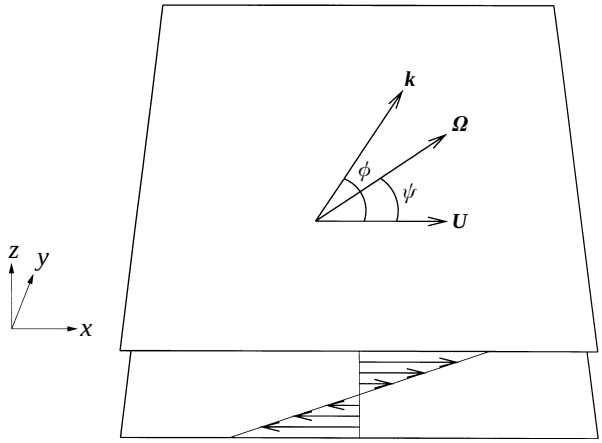

FIGURE 1. The flow geometry. A shear flow is maintained in the x-direction by differential motion of the rigid boundaries at $z = \pm 1/2$. The fluid layer rotates about a horizontal axis that makes an angle ψ with the x-axis. The wavevector of the convection rolls makes an angle ϕ with the x-axis.

becomes

$$(Re\,K\sin\phi + 2\Omega K\cos(\phi-\psi))w = (\mathrm{D}^2 - K^2 - Re\,z\mathrm{i}K\cos\phi)\mathrm{i}\omega, \tag{2.7}$$

$$2\Omega K\cos(\phi-\psi)\mathrm{i}\omega = -RaK^2\theta + (\mathrm{D}^2 - K^2 - Re\,z\mathrm{i}K\cos\phi)(\mathrm{D}^2 - K^2)w, \tag{2.8}$$

$$-w = (\mathrm{D}^2 - K^2 - \sigma Re\,z\mathrm{i}K\cos\phi)\theta. \tag{2.9}$$

Note that when $Re \neq 0$ this eigenvalue problem is not independent of the Prandtl number (Deardorff 1965).

When $\psi = \pm\pi/2$ and buoyancy is ignored, these equations describe the Taylor–Couette problem of flow between concentric cylinders rotating at different rates, in the narrow-gap limit (Chandrasekhar 1961; Busse 1970; Kropp & Busse 1991). The case $\psi = -\pi/2$ corresponds to the potentially unstable situation where the inner cylinder rotates more rapidly than the outer cylinder.

The eigenvalue problem is in general not solvable analytically, and we have resorted to numerical solution, described in §4. There are, however, some results that follow from the symmetries of the problem which are described below. Other analytical results are described in §3.

2.1. *Symmetries and their consequences*

The equations (2.7)–(2.9) have two important symmetries:

(*a*) Rotation of the convection rolls through an angle π about a vertical axis; this corresponds to $\phi \mapsto \phi + \pi$, $(w, \omega, \theta) \mapsto (w, \omega, \theta)^*$, where the asterisk, here and in the remainder of the paper, denotes the complex conjugate.

(*b*) Reflection of the layer in the plane $y = 0$: $\phi \mapsto -\phi$, $\psi \mapsto \pi - \psi$, $\omega \mapsto -\omega$.

Taken together, these symmetries imply that we may restrict attention to $-\pi/2 \leqslant \phi, \psi \leqslant \pi/2$. Note however that unless $\psi = \pm\pi/2$ there is no symmetry under $\phi \mapsto -\phi$ so the growth rate of rolls with a given orientation is generally different from that of their mirror image in a coordinate axis.

These symmetries have implications for the dependence of Ra on the parameters Re, Ω and ϕ. It appears from (2.7)–(2.9) that there is a dependence on $Re\,K\cos\phi$, but this is not consistent with the symmetry $\phi \mapsto \phi + \pi$, so in fact Ra can depend only

on the square of this quantity, $Re^2K^2\cos^2\phi$. After elimination of ω it is found that Ra also depends on the quantities $\Omega^2K^2\cos^2(\phi-\psi)$ and $\Omega ReK^2\cos(\phi-\psi)\sin\phi$. The explicit form of the dependence of Ra on these three combinations of parameters is found analytically for the case of poorly conducting boundaries in §6.

For small values of Re and Ω, it follows that the Rayleigh number is of the form

$$Ra \sim Ra_{RB}(K) + K^2Re^2\left(a_0\cos^2\phi + a_1P\cos(\phi-\psi)\sin\phi + a_2P^2\cos^2(\phi-\psi)\right), \quad (2.10)$$

where $Ra_{RB}(K)$ is the Rayleigh number for Rayleigh–Bénard convection, $P = \Omega/Re$ and the a_i depend on σ. Kropp & Busse (1991) have made a similar expansion for the special case $\psi = \pi/2$, $\phi = 0$. The ratio $P = |\boldsymbol{\Omega}^*|d/U_0^*$ is an inverse Rossby number. Our aim is to minimize Ra over all values of K and ϕ; the values corresponding to the minimum are denoted by Ra_c, K_c and ϕ_c. Minimizing Ra over ϕ, we find from (2.10) that ϕ_c depends only on ψ, the constants a_0, a_1, a_2 and the inverse Rossby number P. K_c may then be found by minimizing Ra over K, and then Ra_c from (2.10). Thus for a fixed value of the ratio P, we expect both ϕ_c and $(Ra_c - Ra_0)/Re^2$ to be independent of Re when Re is small, where $Ra_0 \approx 1707.8$ is the minimum of $Ra_{RB}(K)$ over K.

3. Analysis

We begin by reviewing some results for the case when either the rotation or the shear flow is absent.

In the presence of a moderate shear flow in a non-rotating frame of reference, the preferred mode of convection consists of longitudinal rolls (Ingersoll 1966). These rolls are unaffected by the shear flow, whereas rolls of any other orientation are suppressed.

Similarly, in the absence of an imposed shear flow, a horizontal rotation vector favours rolls aligned with that vector: for $Re = 0$ we expect rolls with $\phi - \psi = \pm\pi/2$. Auer, Busse & Clever (1995) showed that the eigenvalue problem may be reduced to that for Rayleigh–Bénard convection, but with an 'effective Rayleigh number'

$$Ra_{eff} = Ra - 4\Omega^2\cos^2(\phi-\psi). \quad (3.1)$$

In the absence of rotation, the critical Rayleigh number is Ra_0 and the corresponding wavenumber is $K_0 \approx 3.117$ (Chandrasekhar 1961). When $\Omega \neq 0$, it follows that the critical Rayleigh number becomes $Ra_0 + 4\Omega^2\cos^2(\phi-\psi)$. The minimum of this is Ra_0, corresponding to rolls aligned with the rotation vector ($\phi - \psi = \pi/2 \bmod \pi$). The critical wavenumber remains K_0.

3.1. *Rolls with axes aligned with the shear flow*

We now consider the special case of rolls with axes parallel to the direction of the shear flow ($\phi = \pi/2$). We show that for any ψ the eigenvalues of the linear stability problem are real when a certain relation is satisfied by Ω and Re, and that for convenient boundary conditions, the problem reduces to Rayleigh–Bénard convection with a modified Rayleigh number.

The eigenvalue problem (2.4)–(2.6) reduces to

$$(Re + 2\Omega\sin\psi)Kw = (\mathrm{D}^2 - K^2 - \lambda/\sigma)\mathrm{i}\omega, \quad (3.2)$$

$$2\Omega K\sin\psi\,\mathrm{i}\omega = -Ra\,K^2\theta + (\mathrm{D}^2 - K^2 - \lambda/\sigma)(\mathrm{D}^2 - K^2)w, \quad (3.3)$$

$$-w = (\mathrm{D}^2 - K^2 - \lambda)\theta. \quad (3.4)$$

If we multiply these equations by $-\mathrm{i}\omega^*$, w^* and θ^*, respectively, and integrate by parts, using the no-slip and isothermal boundary conditions, we find

$$\begin{aligned} -\mathrm{i}K(Re + 2\Omega\sin\psi)\overline{\omega^* w} &= -\omega_1 - (K^2 + \lambda/\sigma)\omega_0, \\ 2\Omega\mathrm{i}K\sin\psi\,\overline{\omega w^*} &= -Ra\,K^2\overline{\theta w^*} + w_2 + 2K^2 w_1 + K^4 w_0 + (w_1 + K^2 w_0)\lambda/\sigma, \\ -\overline{\theta^* w} &= \theta_1 - (K^2 + \lambda)\theta_0. \end{aligned}$$

The overline indicates an integration in z, and the subscripted variables are defined as follows:

$$w_0 = \overline{|w|^2}, \quad w_1 = \overline{|\mathrm{D}w|^2}, \quad w_2 = \overline{|\mathrm{D}^2 w|^2},$$

with similar definitions for ω_0, ω_1, θ_0 and θ_1. Note that all these subscripted variables are positive definite.

If we now consider the imaginary parts of (3.2)–(3.4) and eliminate the two unknown integrals and their complex conjugates, we are left with

$$\lambda_i\left[2\Omega\sin\psi(Re + 2\Omega\sin\psi)^{-1}\omega_0/\sigma - Ra\,K^2\theta_0 - w_1 - K^2 w_0\right] = 0, \tag{3.5}$$

where λ_i is the imaginary part of λ. Therefore if $Ra > 0$ and $\Omega\sin\psi(Re + 2\Omega\sin\psi) < 0$, the quantity in square brackets is negative and so $\lambda_i = 0$. In this case all eigenvalues (not just those corresponding to marginal modes) are real.

In the case when the growth rate is real, and we seek marginal modes, the variables ω and θ can easily be eliminated from (3.2)–(3.4), simplifying these three equations to

$$(\mathrm{D}^2 - K^2)^3 w + (Ra - 2\Omega\sin\psi(2\Omega\sin\psi + Re))\,K^2 w = 0. \tag{3.6}$$

This is just the usual equation for Rayleigh–Bénard convection, but with an effective Rayleigh number

$$Ra_{eff} = Ra - 2\Omega\sin\psi\,(2\Omega\sin\psi + Re)\,. \tag{3.7}$$

With our choice of boundary conditions the problem can be solved simply by reference to the equivalent (non-rotating) Rayleigh–Bénard problem. For convection in a rotating shear flow, the minimum critical Rayleigh number is therefore

$$Ra = Ra_0 + 2\Omega\sin\psi\,(2\Omega\sin\psi + Re)\,, \tag{3.8}$$

for rolls aligned with the shear flow. This equation shows that convective instability is enhanced if $0 > 2\Omega\sin\psi > -Re$. Since Ω and Re are positive, this enhancement can occur only if $\psi < 0$; this corresponds to the case when the shear flow and the rotation have oppositely directed vorticity. In the special case $\psi = \pi/2$, (3.8) was derived by Kropp & Busse (1991). In the case $\psi = 0$, so the rotation axis and shear flow direction are parallel, (3.8) indicates that the critical Rayleigh number for shear-aligned rolls is the same as that in the absence of either rotation or shear flow.

Another interesting special case of (3.8), considered by Busse (1970), is when there is no convection (i.e. $Ra = 0$) and $\psi = -\pi/2$, in which case the shear flow becomes unstable for a sufficiently large rotation rate, through the Taylor–Couette instability. It can be shown that the usual Taylor number for this problem (Acheson 1990, p. 317) in the limit of a narrow gap can be written as $T = 2\Omega(Re - 2\Omega)$ in our notation, and so the critical Taylor number is $T = Ra_0$.

If we now reintroduce convection then according to (3.8) the onset of instability occurs when $Ra + T = Ra_0$. This equation shows that the Rayleigh–Bénard and Taylor–Couette instabilities add together in a simple way.

3.2. *Rotation vector at right angles to the shear flow*

When $\psi = \pi/2$, the symmetries of the system under (*a*) $\phi \mapsto \phi + \pi$ and (*b*) $(\phi, \psi) \mapsto (-\phi, \pi - \psi)$ imply a symmetry about $\phi = 0$ and about $\phi = \pi/2$. As a consequence, Ra must have a *local* maximum or minimum at $\phi = 0$ and at $\phi = \pi/2$. However, the *global* minimum of Ra may occur for some other orientation (at $\phi = \phi_1$, say, where $\phi_1 \neq 0, \pi/2 \bmod \pi$). In the numerical results presented below, we have found no such ϕ_1; the critical rolls (those which minimize Ra) always have $\phi = 0$ or $\pi/2$ (that is, they are always either longitudinal or transverse). It can be shown from (2.10) that this is the case for small Ω and Re. In other parameter ranges, for example those discussed by Kropp & Busse (1991), oblique rolls may be preferred.

4. Numerical results

In general the eigenvalue problem (2.7)–(2.9) for the critical Rayleigh number must be solved numerically. We describe our numerical solutions in this section. In order to check our numerical results we have used two independent methods, which agree to within an acceptable tolerance. In each case we fix the external parameters (Ω, ψ, Re, σ) and minimize Ra over all values of K and ϕ (or equivalently k and l) to find Ra_c, K_c and ϕ_c.

The first method approximates all functions of z by truncated sums of Chebyshev polynomials and thereby replaces the ordinary differential eigenvalue problem by an algebraic eigenvalue problem involving the coefficients in the sums. Boundary conditions are implemented using the tau method (Gottlieb & Orszag 1977). The calculation is implemented in FORTRAN, and the code is based on a similar code used to solve the linear stability problem for Langmuir circulation (see Cox *et al.* 1992). It has been comprehensively tested against analytical and other numerical results.

The second method uses the dynamical systems package 'AUTO' to solve the boundary-value problem and locate bifurcations from the trivial solution. The critical Rayleigh number is then minimized over k and l in turn by taking the minimum of a quadratic that passes through three different points.

All of our numerical results concern the case of unit Prandtl number ($\sigma = 1$).

We begin by briefly discussing the limiting cases subject to either rotation or shear (but not both); a prior consideration of these will help in interpreting the more general results given below. When $\Omega = 0$ and $Re \neq 0$ the angle ψ is redundant: the critical rolls are aligned with the shear flow ($\phi_c = \pi/2$) and correspond to the expected critical Rayleigh number $Ra_c = Ra_0$. The other limit, in which $Re = 0$ and $\Omega \neq 0$, gives a critical Rayleigh number of Ra_0 for all values of ψ, but $\psi - \phi_c = \pi/2 \bmod \pi$.

4.1. *Dependence of roll orientation on* ψ

For the first set of numerical results we fix the magnitude of the shear flow and the rotation vector (Re and Ω) and calculate the corresponding values of Ra_c, K_c and ϕ_c as functions of the angle ψ between the shear flow and rotation axis. Of particular interest is the variation of ϕ_c with ψ, because this determines the orientation of the critical rolls with respect to the shear flow and the rotation vector. We plot most of our results over the complete range $-\pi < \psi < \pi$ despite the fact only the sub-interval $-\pi/2 < \psi \leqslant \pi/2$ need be considered, in view of the symmetries described in §2. This makes the diagrams easier to analyse. It should also be noted that the angle ϕ has period π; we usually choose it to lie between $-\pi/2$ and $\pi/2$, except when it is more convenient to present a continuous graph avoiding the discontinuities that arise from identifying $\phi = -\pi/2$ with $\phi = \pi/2$.

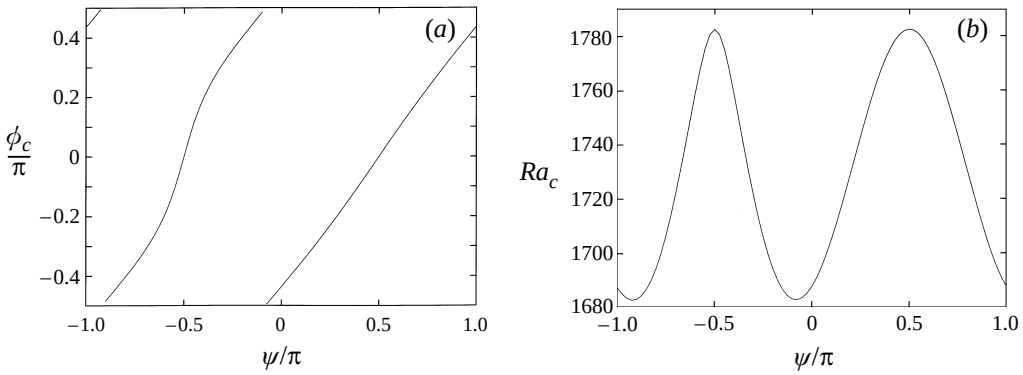

FIGURE 2. (*a*) Plot of ϕ_c against ψ and (*b*) Ra_c against ψ for the case $\Omega = 10$, $Re = 10$.

We now introduce a 'winding number' associated with the stability problem. We imagine increasing ψ through 2π radians and tracking the corresponding values of ϕ_c. If ϕ_c varies continuously with ψ then it will increase by an well-defined integer multiple of π, say $n\pi$, as ψ rotates through 2π. We define the winding number to be $\mathcal{N} = n/2$. Although in the two limiting cases described above each graph of ϕ_c against ψ is quite trivial in itself, it is noteworthy that the 'winding number' in the shear-only case is zero (the rolls always point in the same direction) while that in the 'rotation-only' case is 1 (the orientation of the critical rolls rotates through a full circle as the orientation of the rotation vector does the same). Since the winding number can be only integer multiples of $\frac{1}{2}$, we expect discontinuous changes in $\mathcal{N}$ and hence in the topology of the graph of ϕ_c against ψ as the problem is varied smoothly between the two limiting cases. (The book by Winfree (1980) contains many examples of the use of a winding number in biological systems, and we recommend to the reader his discussion of phase singularities in maps.)

We first fix $\Omega = 10$ and solve the linear stability problem for a range of values of Re. When $Re = 10$ (see figure 2), the rotation dominates and the topology of $\phi_c(\psi)$ is the same as for $Re = 0$, with $\mathcal{N} = 1$. When $Re = 20$, however, $\mathcal{N} = \frac{1}{2}$ and a change in the topology has taken place (see figure 3). As ψ is varied through the half-circle from $-\pi$ to 0, the rolls remain approximately aligned with the shear flow, and only when ψ is increased from 0 to π are the rolls roughly aligned with the rotation. We can relatively easily determine the critical Reynolds number Re_- at which the change in topology takes place as follows. We first note that at $\psi = -\pi/2$, ϕ_c is either 0 (for $Re < Re_-$ and $\mathcal{N} = 1$) or $\pi/2$ (for $Re > Re_-$ and $\mathcal{N} = \frac{1}{2}$). We therefore need only compare the values of the corresponding Rayleigh numbers; they will be equal at $Re = Re_-$. We find numerically that $Re_- \approx 13.35$. Two cases near $Re = Re_-$ are shown in figure 4. Note that in the neighbourhood of $Re = Re_-$ and $\psi = -\pi/2$, the orientation ϕ_c depends very sensitively on ψ. For example, in each of the curves of figures 4 there is a jump in ϕ_c between $\pm\pi/4 \bmod \pi$ corresponding to a very small change in ψ. We return to this point at the end of §6.

There is a second change in the winding number, from $\frac{1}{2}$ to 0, at $Re = Re_+ \approx 42.3$: for $Re \approx Re_+$ the orientation ϕ_c is now a very sensitive function of ψ near $\psi = \pi/2$. For $Re > Re_+$ the rolls are roughly aligned with the shear flow regardless of the direction of the rotation vector. Results for $Re = 50 > Re_+$ are shown in figure 5.

Given the arguments at the end of §2.1, we expect that for small Re and Ω, and a fixed value of the ratio $P = \Omega/Re$, ϕ_c and $(Ra_c - Ra_0)/Re^2$ are independent of Re.

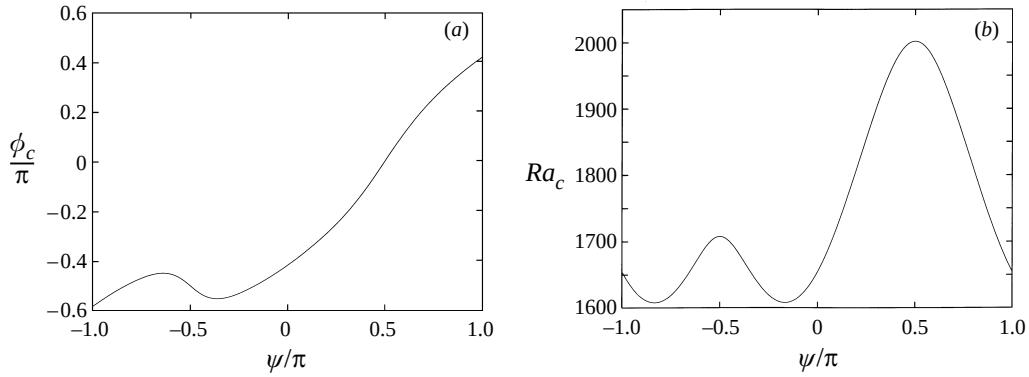

FIGURE 3. (*a*) Plot of ϕ_c against ψ and (*b*) Ra_c against ψ for the case $\Omega = 10$, $Re = 20$.

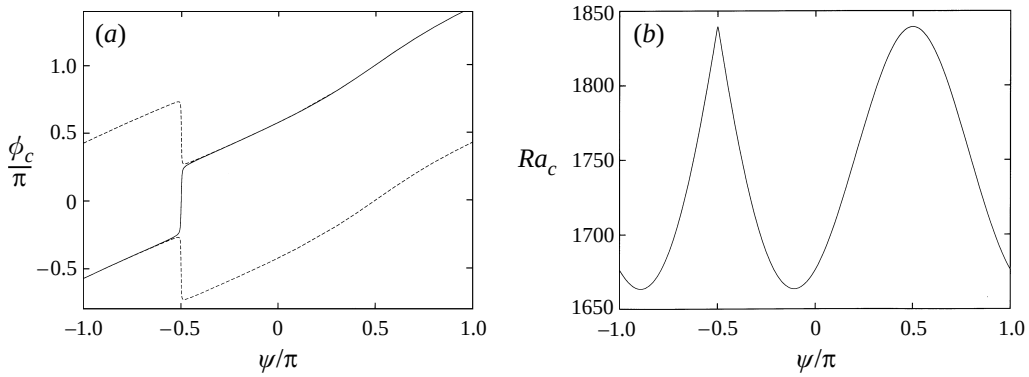

FIGURE 4. (*a*) Plot of ϕ_c against ψ. Solid line $Re = 13.3$, with $\mathcal{N} = 1$; dashed line $Re = 13.4$, with $\mathcal{N} = \frac{1}{2}$. Note that the data for $Re = 13.4$ have been plotted twice (recall that ϕ and $\phi + \pi$ represent the same convection rolls), to show that there is a significant difference between the values of ϕ_c in the two cases only near $\psi = -\pi/2$. (*b*) Plot of Ra_c against ψ for $\Omega = 10$, $Re = 13.3$ (the plot for $Re = 13.4$ is virtually identical).

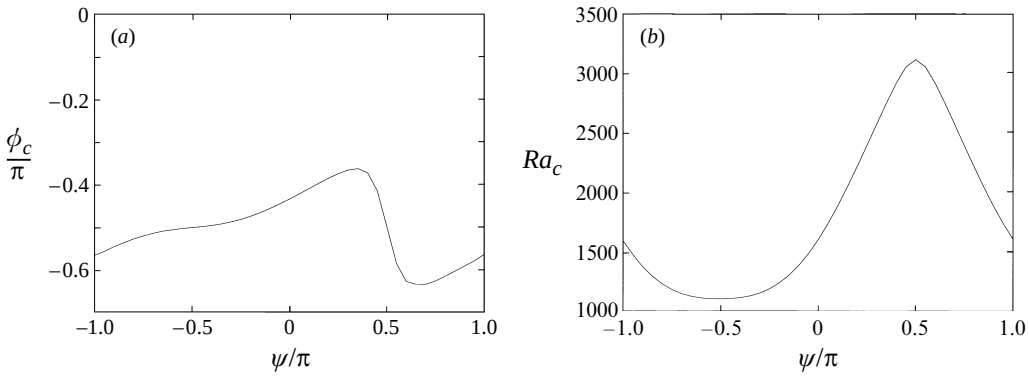

FIGURE 5. (*a*) Plot of ϕ_c against ψ and (*b*) Ra_c against ψ for the case $\Omega = 10$, $Re = 50$.

To show that this is indeed the case we have plotted on figure 6 four sets of data for $P = 0.5$, corresponding to $\Omega = 1$, 5, 10 and 20. As can be seen, even for $\Omega = 20$ (and hence $Re = 40$) this small-Re asymptotic result still holds to a good approximation. We also expect the winding number $\mathcal{N}$ to depend on Ω and Re only through their ratio, when both are small. For larger values of the rotation rate, however, these scalings no longer apply: a calculation for $\Omega = 100$, $Re = 200$ (where $P = 0.5$) yielded results qualitatively similar to those of figure 2 (where $P = 1$), whereas the small-Re asymptotic result predicts similarity to figure 3.

4.2. *Aligned rotation and shear flow*

We now consider in more detail the case when the shear flow and rotation vector are aligned ($\psi = 0$). If either Ω or Re is zero, we expect the convection rolls to share this alignment, i.e. $\phi_c = \pi/2$, as discussed in §3. At first sight it may seem that since both rotation and shear flow individually favour aligned rolls, the combination of the two will have the same effect. Busse & Kropp (1992) discovered the remarkable fact that this is not the case, and in fact the preferred mode of convection consists of rolls with their axes at a slight angle to the direction of $\boldsymbol{\Omega}$ and $\boldsymbol{U}_0$. A similar phenomenon also occurs for Poiseuille flow in a rotating pipe (Pedley 1969; Joseph & Carmi 1969). The reason for this is the symmetry-breaking induced by the combination of shear and rotation. As discussed in §2.1, there is no symmetry under reflection in the coordinate axes ($\phi \mapsto -\phi$) when Ω and Re are both non-zero. Ra depends on $Re^2 K^2 \cos^2\phi$, $\Omega^2 K^2 \cos^2\phi$ and $\Omega Re K^2 \cos\phi \sin\phi$. Since both odd and even functions of ϕ appear in the eigenvalue problem for Ra, generically there is no reason to expect Ra to be a minimum at $\phi = \pi/2$.

Figure 7 shows the dependence of ϕ_c and Ra_c on Ω for $Re = 20$. As expected, $\phi_c \to -\pi/2$ and $Ra_c \to Ra_0$ as $\Omega \to 0$. As Ω increases, the alignment of the roll axis departs from that of the shear flow, reaching a maximum of 15°, and then returns to $-\pi/2$ as $\Omega \to \infty$. The critical Rayleigh number decreases monotonically as Ω increases, and does not return to 1707.8 as $\Omega \to \infty$ but instead approaches a limit of 1607.8.

This behaviour can be explained by the following asymptotic argument. We seek a scaling in which $\phi = \pi/2 + \epsilon$ as $\Omega \to \infty$, where ϵ is small. Substituting this scaling into the equations (2.7)–(2.9) with $\psi = 0$, and discarding terms of $O(\epsilon)$ but retaining those of $O(\Omega\epsilon)$, the terms in $Re\cos\phi$ disappear. This means that θ and ω can be eliminated (following the method of §3.1), to give the single equation for w,

$$(\mathrm{D}^2 - K^2)^3 w + (Ra + 2\Omega\epsilon(Re - 2\Omega\epsilon))\, K^2 w = 0. \tag{4.1}$$

Once again, the usual Rayleigh–Bénard problem appears, with an effective Rayleigh number

$$Ra_{eff} = Ra + 2\Omega\epsilon\,(Re - 2\Omega\epsilon)\,, \tag{4.2}$$

and the solution is therefore $Ra_{eff} = Ra_0$, $K = K_0$. Ra_c and ϵ are determined by minimizing Ra over ϵ, which gives $\epsilon = Re/4\Omega$ and $Ra_c = Ra_0 - Re^2/4$. These asymptotic results are plotted with the numerical solutions in figure 7.

Similar behaviour is found when the Reynolds number is varied at a fixed rotation rate. For example, when $\psi = 0$ and $\Omega = 10$, we find that $Ra_c \to Ra_0$ as $Re \to 0$, but $Ra_c \to 1573$ as $Re \to \infty$. When $\Omega = 20$ instead, the limit is $Ra_c \to 1154$ as $Re \to \infty$. In a similar fashion to the analysis described above, it is possible to find a distinguished limit in which $\phi = \pi/2 + \epsilon$ and $Re = O(\epsilon^{-1})$. However, the limiting eigenvalue problem that results cannot be reduced to the standard Rayleigh–Bénard

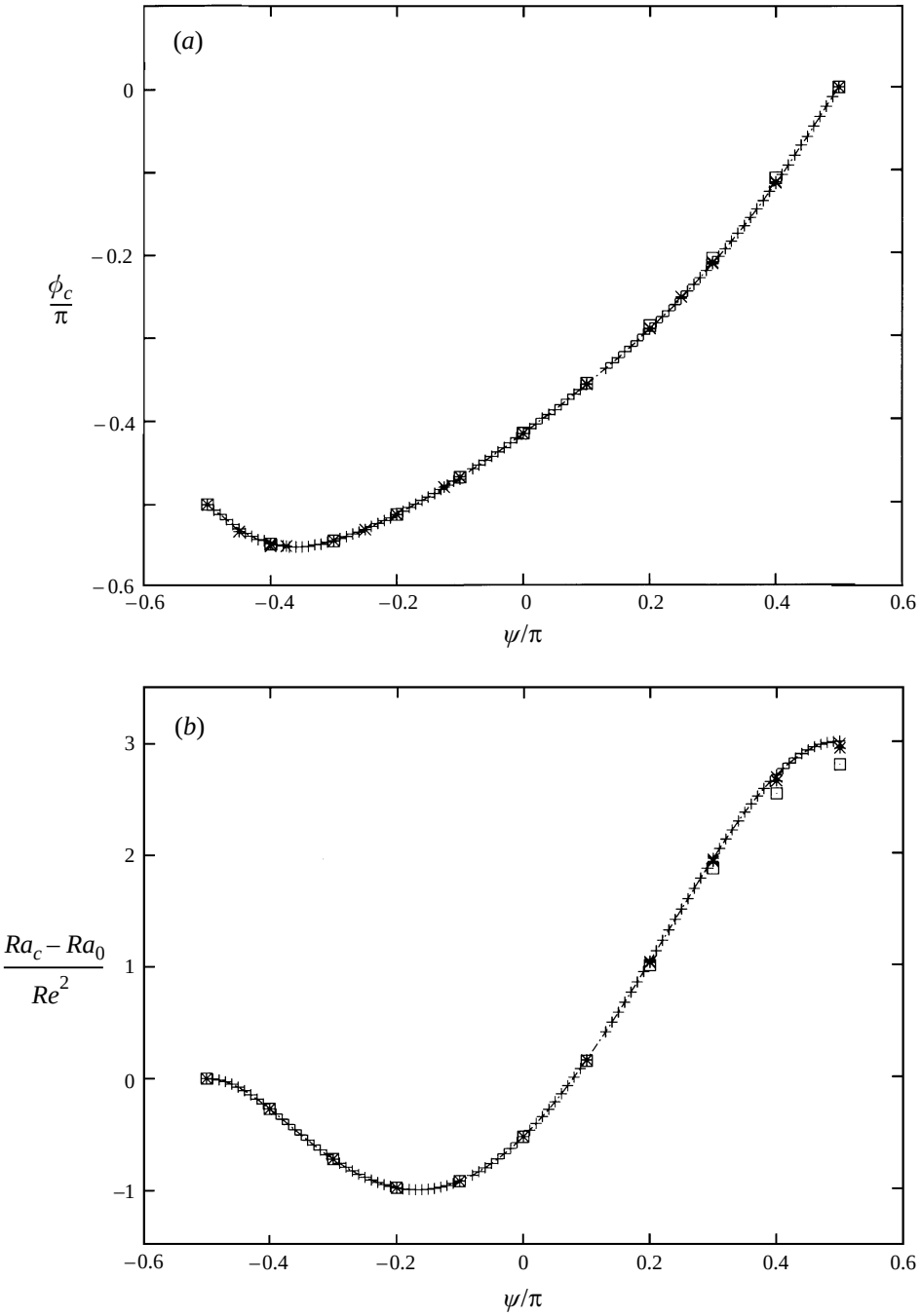

FIGURE 6. (*a*) Plot of ϕ_c against ψ and (*b*) $(Ra_c - Ra_0)/Re^2$ against ψ for the case $P = 0.5$. Line and $\diamond$, $\Omega = 1$; $+$, $\Omega = 5$; $\square$, $\Omega = 10$; $\times$, $\Omega = 20$.

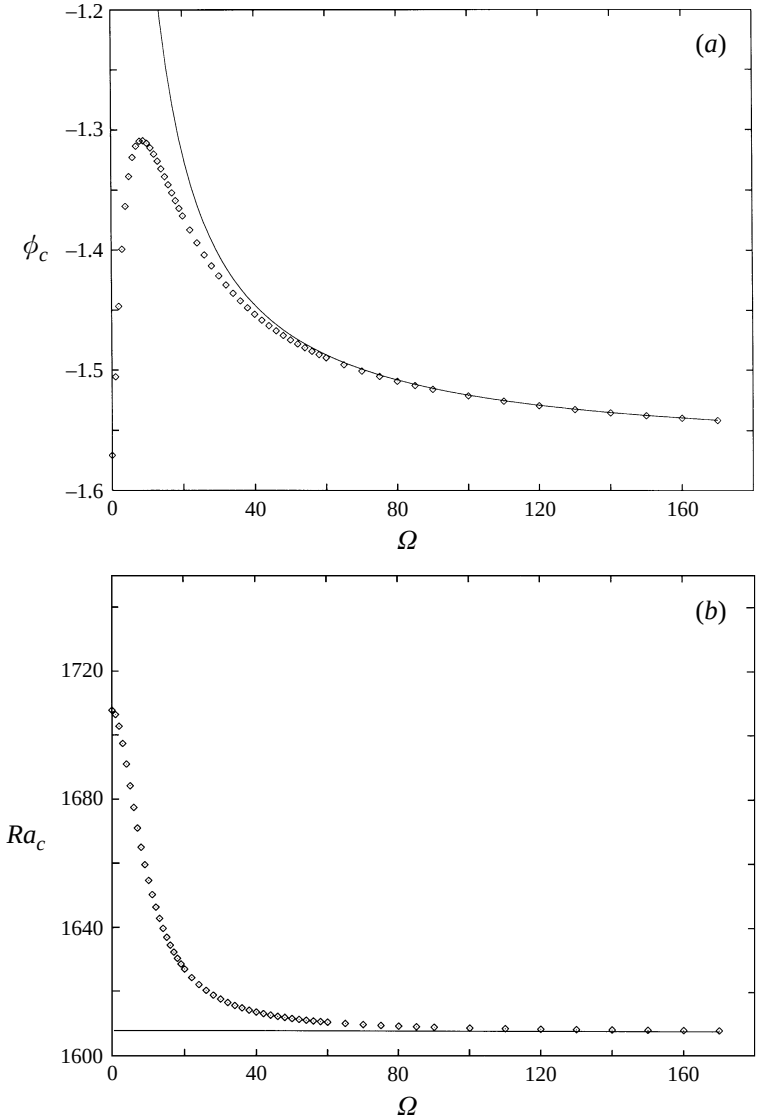

FIGURE 7. Dependence of (*a*) ϕ_c and (*b*) Ra_c on Ω for the case $\psi = 0$, $Re = 20$, showing agreement between numerical solution (points) and the asymptotic prediction (line).

problem with a modified Rayleigh number and we have been unable to determine analytically as a function of Ω the limiting value of Ra_c as $Re \to \infty$.

5. Nonlinear behaviour

In this section we present some fully nonlinear numerical simulations for convection in a rotating shear flow. The simulations are intended to illustrate some of the behaviour possible in the fluid layer. A full analysis of the various solution branches, their stability and bifurcations would be a huge undertaking, not attempted here. The results were obtained from a pseudo-spectral code which uses Fourier modes in the

ψ	Ra_c	Ra	Nu	Description
$-\pi/2$	1708	1800	1.0733	rolls with $\phi = \pi/2$
		1900	1.1458	rolls with $\phi = \pi/2$
		2000	1.2120	rolls with $\phi = \pi/2$
		2100	1.2728	rolls with $\phi = \pi/2$
		2200	1.3289	rolls with $\phi = \pi/2$
		2200	1.3025	defect
0	1655	1750	1.0716	rolls with $\phi = -1.37$
		1850	1.1443	rolls with $\phi = -1.37$
		1950	1.2107	rolls with $\phi = -1.37$
		2200	1.3546	rolls with $\phi = -1.37$
$\pi/2$	2001	2100	1.0411	wavy rolls
		2200	1.004–1.112	oscillatory wavy rolls

TABLE 1. Summary of nonlinear results

horizontal directions and Chebyshev polynomials in the vertical direction. Further details of the numerical method can be found elsewhere (Cox & Matthews 1997).

The simulations were carried out with rigid, fixed-temperature upper and lower boundaries, in a rectangular box of size $10 \times 10 \times 1$ with periodic boundary conditions in the horizontal directions. Since the preferred wavenumber in the absence of shear flow or rotation is $K_0 \approx 3.117$, the preferred wavelength of a pair of rolls is 2.016 and so the box size allows 5 pairs of rolls. The box size, together with the periodic boundary conditions, imposes some constraints on the permissible roll orientation ϕ, but it is sufficiently large that these constraints are not too restrictive. The numerical resolution used was $48 \times 48 \times 33$. The initial condition used was the equilibrium configuration plus a small random perturbation to each Fourier mode. The computations were continued until a steady or periodic pattern emerged.

Results were obtained for the parameter values $\sigma = 1$, $Re = 20$, $\Omega = 10$, for comparison with figure 3, with $\psi = -\pi/2$, 0 and $\pi/2$. Several runs were carried out at different Rayleigh numbers and these are summarized in table 1, which gives the Nusselt number Nu and a qualitative description for each run. The solution obtained at $Ra = 2200$ is illustrated in figure 8 for each value of ψ.

For $\psi = -\pi/2$ (rotation perpendicular to the shear flow with oppositely directed vorticity) our linear theory shows that convection rolls with axes aligned with the shear flow have the lowest critical Rayleigh number ($\phi_c = \pi/2$). For these rolls the analysis of §3.1 applies, and the critical Rayleigh number is Ra_0 since for these parameter values the effects of the rotation and shear flow cancel in (3.8). Our simulations show that aligned rolls are indeed obtained in the nonlinear regime. The dependence of $Nu - 1$ on $Ra - Ra_c$ is linear, strongly suggesting that the bifurcation is supercritical. The bifurcation may be subcritical for small Prandtl numbers (Kropp & Busse 1991) or for strong shear flows (Clever & Busse 1992). One computation at $Ra = 2200$ shows a pattern that consists predominantly of aligned rolls, but with a defect. Figure 8(*a*) shows this solution in the form of an isosurface of the vertical velocity w viewed from above. Dark areas indicate rising fluid. On the time scale of our integrations, this defect appears to be a stable stationary solution of the equations; the integration was continued for 70 time units which corresponds to several hundred convective turnover times. For nonlinear convection in a large box, it is to be expected that there

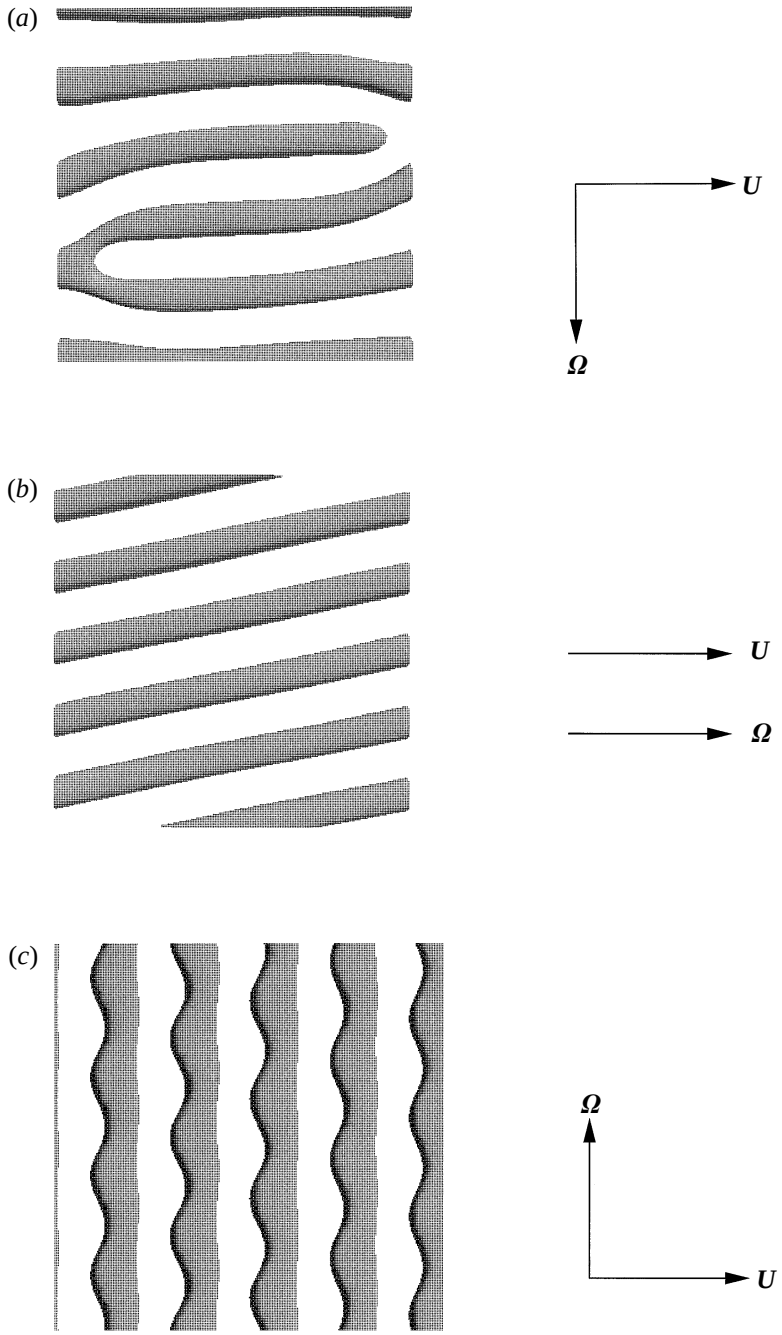

FIGURE 8. Numerical solutions of the fully nonlinear governing equations for convection with $Re = 20$, $\Omega = 10$, $Ra = 2200$, for (*a*) $\psi = -\pi/2$, (*b*) $\psi = 0$, (*c*) $\psi = \pi/2$.

may be several stable solutions. The computation was repeated with a different initial condition, and a stable solution was found with perfectly aligned rolls.

For $\psi = 0$ (rotation parallel to the shear flow, figure 8*b*) rolls appear at a slight angle to the shear flow. The predominant Fourier mode is the $(-1, 5)$ mode, so the angle ϕ is $\tan^{-1}(-5) = -1.37$. This agrees well (subject to the restriction imposed by the finite box size) with the result predicted by linear theory, $\phi_c = -1.31$.

Finally, with $\psi = \pi/2$ (rotation perpendicular to the shear flow with vorticity in the same direction) the linear theory predicts rolls with axes aligned with the rotation vector ($\phi_c = 0$, figure 3). The nonlinear results (figure 8*c*) are in agreement, showing roll axes aligned with the rotation, but the rolls have a wavy appearance. For $Ra = 2100$ steady wavy rolls occur, with four waves on each roll. Similar wavy rolls were found by Auer *et al.* (1995) in a system of amplitude equations for convection in a rotating annulus with differentially heated sidewalls. They describe the pattern as having 'a varicose deformation of the roll pattern which shifts by half a wavelength along the axis of the rolls from one pair of rolls to the next'. In our simulation, this shift is three-fifths of a wavelength, but this figure is dependent on the box size: in a larger box we have found a shift of half a wavelength. This pattern can be interpreted as an interaction between three Fourier modes with phases that sum to π, so that with three equal amplitudes the pattern would appear triangular. For $Ra = 2200$ the convection is oscillatory: straight rolls become unstable to a wavy instability which increases in amplitude until the pattern resembles triangles; these then revert to straight rolls again, with a period of 4.3 time units.

6. Poorly conducting boundaries

The boundary conditions we have chosen limit the analytical progress that can be made with (2.7)–(2.9). However, in convection problems there are two common choices of alternative boundary conditions that allow more progress to be made. The first, when applied to the Rayleigh–Bénard problem, considers the horizontal boundaries to be stress-free and isothermal, with the consequence that the eigenfunctions are trigonometric functions of z and the eigenvalue problem can be completely solved analytically. A shear flow generated by a constant stress at each horizontal boundary leaves the boundary conditions on perturbations unaltered, but the eigenvalue problem can no longer be solved in closed form in the presence of the shear flow; it is similarly complicated by the presence of rotation. This alternative set of boundary conditions therefore provides no assistance. The second common choice of boundary conditions concerns a layer of fluid confined between boundaries that conduct heat more poorly than the fluid itself. In this case the problem of convection in the fluid should properly be coupled to that of heat conduction in the boundaries. A simpler approach, adopted here, is to apply a model boundary condition on the temperature inspired by Newton's law of cooling, so that

$$\frac{\partial T}{\partial z} + \alpha_+ T = T_+, \quad \frac{\partial T}{\partial z} - \alpha_- T = T_-$$

at the upper and lower boundaries, respectively. For poorly conducting boundaries, α_+ and α_- are small non-negative constants, in which case the first modes to become unstable have small wavenumbers k and l. In this circumstance, the linear stability theory may be solved exactly by a long-wave perturbation analysis. This was first done in the absence of shear and rotation by Busse & Riahi (1980), who also considered the weakly nonlinear regime. Chapman & Proctor (1980) derived a weakly nonlinear

long-wave partial differential equation to describe convection in the same problem. Weak shear was incorporated into the analysis by Cox (1996, 1997).

In the absence of shear and rotation, a distinguished limit may be obtained in which $K = O(\epsilon)$, $\alpha = O(\epsilon^4)$ and $r = O(\epsilon^2)$, where $\alpha = \alpha_+ + \alpha_-$ and r is the scaled Rayleigh number $r = Ra/720 - 1$. The growth rate is then (Busse & Riahi 1980; Chapman & Proctor 1980; Proctor 1981)

$$\lambda \sim -\alpha + rK^2 - aK^4 = O(\epsilon^4),$$

where $a = 17/462$. The growth rate is independent of ϕ; there is no preferential orientation of the rolls. The dominant effect of introducing a non-zero shear flow is to add to λ a term $-Re^2k^2/120$ (Cox 1996, 1997). If $Re = O(1)$ then this 'shear dispersion' term is $O(\epsilon^2)$, and dominates the contributions to λ. It can, however, be balanced with the terms of $O(\epsilon^4)$ by assuming that the shear flow is weak, with $Re = O(\epsilon)$. If this scaling is adopted and $\Omega = O(1)$, the growth rate is then

$$\lambda \sim -\alpha + rK^2 - aK^4 - eRe^2K^2\cos^2\phi - \frac{2b\Omega^2}{\sigma^2}K^4\cos^2(\psi - \phi) = O(\epsilon^4),$$

where $e = 1/120$ and $b = 131/332640$. Although all terms in λ are of the same formal order in ϵ, this expression is unsatisfactory because Re and Ω occur only quadratically, whereas we know that there is no such symmetry $Re \mapsto -Re$ or $\Omega \mapsto -\Omega$ in the full problem. (It turns out that at higher order in ϵ these symmetries are broken.)

In order to derive an expression for λ which does not have the shortcoming indicated above, we suppose that Re and Ω are each $O(1)$ and derive the first two terms in an asymptotic expansion of the growth rate $\lambda \sim \epsilon^2\lambda_2 + \epsilon^4\lambda_4$, truncating this expansion at $O(\epsilon^4)$. The growth rate is then

$$\begin{aligned}\lambda = {} & -eRe^2K^2\cos^2\phi - \alpha + rK^2 - aK^4 + dRe^2K^4\cos^2\phi - cRe^4K^4\cos^4\phi \\ & - \frac{b\Omega}{\sigma^2}\left[Re\sin\phi + 2\Omega\cos(\psi - \phi)\right]K^4\cos(\psi - \phi),\end{aligned} \tag{6.1}$$

where

$$c = \frac{59}{9979200}, \quad d = \frac{716\sigma + 4538\sigma^2 - 5}{4656960\sigma^2}.$$

The first term is formally $O(\epsilon^2)$, while all others are $O(\epsilon^4)$. Despite this mixing of scales, we treat (6.1) as an exact formula for the growth rate, valid in the limit as $K, \alpha \to 0$, and explore its consequences below. We expect this procedure to be most reasonable for small Re and Ω and to make analytical progress we apply a further approximation, namely that we retain only those terms quadratic in these quantities, and drop the quartic term in Re. For the remainder of this paper we therefore set $c = 0$. Note that the form of the dependence of λ on the parameters is exactly as predicted by the symmetry arguments of §2.1.

It remains to be shown that the truncation (6.1) provides a good approximation to the true growth rate. We have therefore compared the marginal stability curve found by solving (2.7)–(2.9) numerically with that obtained by setting $\lambda = 0$ in (6.1). We find generally good agreement when α is small and provided Re and Ω are not too large. (As a rough rule of thumb, for $\alpha = 0.01$ we found that agreement was good for Re and Ω around 1, and poor for Re and Ω around 5.) It is not our intention to offer an exhaustive evaluation of the truncation (6.1); it suffices to say that despite its limitations it provides some analytical insight into the linear stability problem that does not seem to be obtainable more directly.

For given values of the parameters Re, Ω, ψ and σ, we may calculate the scaled critical Rayleigh number r_c by solving $\lambda = 0$ for r, where λ is given by (6.1), then minimizing this value of r over all values of K and ϕ. However, we find it easier to seek stationary points of λ, that is, where $\lambda = \partial\lambda/\partial K = \partial\lambda/\partial\phi = 0$. Of course, there may be more than one such stationary point, and we need to check which corresponds to a global minimum of r. The critical wavenumber K_c may be obtained by considering $K\partial\lambda/\partial K - 2\lambda = 0$, from which it follows that

$$K_c^4 = \alpha \left[a - dRe^2 \cos^2\phi_c + \frac{b\Omega}{\sigma^2}\,(Re \sin\phi_c + 2\Omega\cos(\psi - \phi_c))\cos(\psi - \phi_c) \right]^{-1}. \quad (6.2)$$

Substitution of this expression into $\partial\lambda/\partial\phi = 0$ yields an equation for the corresponding value of ϕ_c:

$$e^2 Re^4 \sin^2 2\phi_c = K_c^4 \left[dRe^2 \sin 2\phi_c + \frac{b\Omega}{\sigma^2}(Re\cos(\psi - 2\phi_c) + 2\Omega \sin 2(\psi - \phi_c)) \right]^2, \quad (6.3)$$

with K_c^4 given in (6.2). If we retain only the leading-order contributions of shear and rotation, consistent with the approximations made in deriving (6.2) and (6.3), ϕ_c may be obtained explicitly from these equations, and after some manipulation we find

$$(E - FP\,[\sin\psi - 2P\cos 2\psi])\tan 2\phi_c = FP\cos\psi(1 + 4P\sin\psi), \quad (6.4)$$

where

$$E = e - d(\alpha/a)^{1/2}, \quad F = b(\alpha/a)^{1/2}/\sigma^2 \quad \text{and} \quad P = \Omega/Re.$$

As one might expect, given the approximations made thus far, the stability problem depends on Ω and Re only through their ratio P. This is not true of the problem with isothermal boundaries (2.7)–(2.9), although we saw that it is true in the limit as $Re \to 0$. This equation for ϕ_c has two solutions in the range $-\pi/2 < \phi_c \leqslant \pi/2$: ϕ_1 which lies in the range $-\pi/4 < \phi \leqslant \pi/4$, and ϕ_2 which satisfies $|\phi_2 - \phi_1| = \pi/2$. Since the difference between ϕ_1 and ϕ_2 is $\pi/2$, the two solutions represent orthogonal sets of rolls, one corresponding to a saddle point of r and one to a minimum. The scaled Rayleigh number r_c may likewise be calculated, retaining only the leading-order contributions of shear and rotation, to give

$$\begin{aligned} r_c &= \left(\frac{\alpha}{a}\right)^{1/2} \left\{ 2 + \left[-\tfrac{1}{2}d + \frac{bP}{\sigma^2}\left(\tfrac{1}{2}\sin\psi + P\right) \right] Re^2 \right\} + \tfrac{1}{2}eRe^2 \\ &\quad + \tfrac{1}{2}Re^2 \left(\frac{\alpha}{a}\right)^{1/2} \frac{bP}{\sigma^2}\cos\psi(1 + 4P\sin\psi)\operatorname{cosec} 2\phi_c \\ &\equiv r_0 + \tfrac{1}{2}Re^2 FP\cos\psi(1 + 4P\sin\psi)\operatorname{cosec} 2\phi_c. \end{aligned} \quad (6.5)$$

To select the correct root ϕ_1 or ϕ_2 we first calculate the corresponding Rayleigh numbers r_1 and r_2 from (6.5) and then choose the lower of these two values. This procedure corresponds to choosing ϕ_c such that

$$P\cos\psi(1 + 4P\sin\psi)\operatorname{cosec} 2\phi_c < 0.$$

It is instructive to examine the limits in which shear or rotation dominate.

In the former case, $P \to 0$ and (6.4) reduces to $\tan 2\phi_c \sim 0$, so either $\phi_c \sim 0 \bmod \pi$ (transverse rolls) or $\phi_c \sim \pi/2 \bmod \pi$ (longitudinal rolls). The corresponding Rayleigh number is

$$r_c \sim r_0 + \tfrac{1}{2}Re^2 E\cos 2\phi_c,$$

and so the longitudinal rolls are the first to grow, while the transverse rolls are the most stable, provided $E > 0$. This inequality corresponds to ensuring that α is small enough for the long-wave expansion, which is predicated on the smallness of α, to be valid. We assume it to hold, in which case our physical intuition is confirmed by the long-wave analysis: rolls aligned with the shear flow are preferred when the shear flow dominates over rotation.

In the latter case, $P \to \infty$ and (6.4) becomes $\tan 2\phi_c \sim \tan 2\psi$, so that $\psi - \phi_c \sim 0 \bmod \pi$ (rolls with axes aligned at right angles to the rotation vector) or $\psi - \phi_c \sim \pi/2 \bmod \pi$ (axes parallel to the rotation vector). The critical Rayleigh number is

$$r_c \sim r_0 + \Omega^2 F \frac{\cos 2\psi}{\cos 2\phi},$$

which indicates that, as expected, rolls with axes aligned in the direction of the rotation vector are preferred.

It is tempting to extend analysis of these limits to explain results analogous to those of §4.2 for large Ω or Re in the context of the long-wave model. However, it should be recalled that an assumption has been made in deriving the long-wave theory that Re and Ω are not too large; the limits as $Re \to \infty$ or $\Omega \to \infty$ cannot, therefore, be treated.

Some other special cases are of interest. For example, when the angular velocity vector and the shear flow are aligned ($\psi = 0$ or π) we can find bounds on the deviation of the critical rolls from alignment with the shear flow. In this case, we have, from (6.4) and (6.5),

$$\tan 2\phi_c = \frac{FP \cos\psi}{E + 2FP^2}$$

and

$$r_c = r_0 + \tfrac{1}{2} Re^2 (E + 2FP^2) \sec 2\phi_c.$$

The rolls corresponding to a minimum of r can easily be determined by noting that $\sec 2\phi > 0$ for $0 \leqslant |\phi| < \pi/4$ and $\sec 2\phi < 0$ for $\pi/4 < |\phi| < \pi/2$. Therefore the minimum value of r corresponds to some ϕ_c in the range $\pi/4 < |\phi_c| \leqslant \pi/2$, with equality only if $P = 0$ or ∞. Since r_c may also be written as

$$r_c = r_0 + \tfrac{1}{2} Re^2 FP \cos\psi \operatorname{cosec} 2\phi_c,$$

we see that at a minimum of r, ϕ_c and $P \cos\psi$ must have opposite signs when P is non-zero and finite. Furthermore, since the maximum value of $FP/(E + 2FP^2)$ is $(F/(8E))^{1/2}$, we can improve the bounds on ϕ_c: the true bounds are

$$\frac{\pi}{2} - \frac{1}{2} \tan^{-1} \left(\frac{F}{8E} \right)^{1/2} \leqslant |\phi_c| \leqslant \frac{\pi}{2},$$

with equality at the lower bound corresponding to $2P^2 = E/F$, and at the upper to $P = 0$ or ∞. The maximum deviation of the rolls from alignment with the x-axis is therefore $\frac{1}{2} \tan^{-1}(F/(8E))^{1/2}$.

When instead the angular velocity vector lies at right angles to the shear flow ($\psi = \pm\pi/2$), we find

$$(E - FP(\pm 1 + 2P)) \tan 2\phi_c = 0,$$

so that $\phi_c = 0$ or $\pi/2$ unless the prefactor of $\tan 2\phi_c$ is zero, in which case ϕ_c is

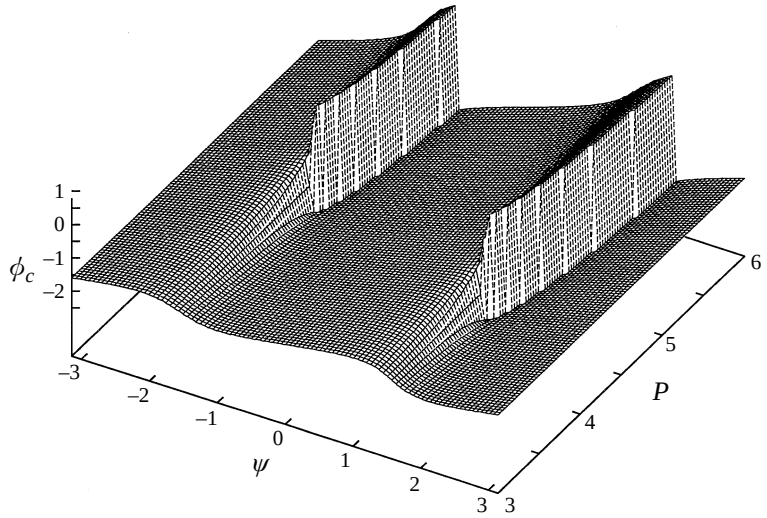

FIGURE 9. ϕ_c plotted as a function of ψ and P for $\alpha = 0.01$, $\sigma = 1$. This surface shows the changes in winding number $\mathcal{N}$ as P is varied.

undefined. The corresponding Rayleigh number is

$$r_c = r_0 + \tfrac{1}{2}Re^2(E - FP(\pm 1 + 2P))\sec 2\phi_c.$$

We consider the two choices of ψ separately. When $\psi = -\pi/2$, $\phi_c = 0$ if $E - FP(2P - 1) < 0$ and $\phi_c = \pi/2$ if the inequality is reversed. Since $P \geqslant 0$, the inequality is satisfied when $P > P_+$, where P_+ is the positive root of

$$2FP^2 - FP - E = 0. \tag{6.6}$$

In other words, when rotation dominates the critical roll axes are aligned with the rotation vector. Otherwise they align with the shear flow. When $\psi = \pi/2$, $\phi_c = 0$ if $E - FP(2P + 1) < 0$ and $\phi_c = \pi/2$ if the inequality is reversed. Now the inequality is satisfied if $P > -P_-$, where $P_- > -P_+$ is the negative root of (6.6), that is, if the rotation dominates.

In our numerical results for rigid, isothermal boundaries we found a discontinuous change in the topology of the graph of ϕ_c against ψ at certain parameter values (i.e. a change in the winding number). In the long-wave model, a similar discontinuity takes place when $P = P_+$ or $-P_-$. To analyse the discontinuities, we suppose that P is close to one of the threshold values, and examine the corresponding neighbourhood of either $\psi = -\pi/2$ or $\psi = \pi/2$ by setting

$$\psi = \psi_0 + \delta\psi_1 \quad \text{and} \quad P = P_0 + \delta P_1,$$

where $(P_0, \psi_0) = (-P_-, -\pi/2)$ or $(P_+, \pi/2)$. In either event (6.3) becomes

$$\tan 2\phi_c \sim \frac{P_0\psi_1}{P_1}.$$

This equation indicates that for values of (P, ψ) near either of the (P_0, ψ_0) there is a 'boundary layer' in the graph of ϕ_c in which ϕ_c adjusts from its value at ψ_0 to $\pm\pi/4 \bmod \pi$. The details are as follows. For a fixed value of P_1 (that is, for fixed Ω and Re near the threshold for a discontinuity in $\mathcal{N}$), $\phi_c \to \pi/4$ as $\psi_1 \to \infty$ (that is, just to the right of $\psi = \psi_0$) and $\phi_c \to -\pi/4$ as $\psi_1 \to -\infty$ (just to the left of

$\psi = \psi_0$). Of course the two cases $P_1 < 0$ and $P_1 > 0$ are quite different because (at ψ_0) $\phi_c = \pi/2$ in the former and $\phi_c = 0$ in the latter.

Figure 9 shows ϕ_c plotted as a function of ψ and P for the case $\alpha = 0.01$ and $\sigma = 1$. Other choices of these parameters give qualitatively similar plots. For sufficiently small values of P (towards the front of the surface), ϕ_c is approximately independent of ψ and $\mathscr{N} = 0$, while for large P (towards the back), $\phi_c - \psi$ is approximately independent of ψ and $\mathscr{N} = 1$. The two discontinuities can clearly be seen, at $P = 4.10$ and 4.60.

7. Conclusions

We have considered the onset of convection in a rotating fluid layer confined between isothermal, rigid boundaries which are in differential motion. In a limited number of particular cases, analytical progress has been possible, building on the work of Busse and co-workers (Busse 1970; Kropp & Busse 1991; Busse & Kropp 1992; Auer *et al.* 1995), by reducing the problem to an equivalent eigenvalue problem resembling that of standard Rayleigh–Bénard convection, but with a modified Rayleigh number. We confirm the unexpected result of Busse & Kropp (1992) that when the shear flow and rotation vector are parallel, oblique rolls are preferred and the critical Rayleigh number is reduced.

A change in the thermal boundary condition to simulate poorly conducting boundaries allows greater analytical progress; in particular, it allows the critical Rayleigh number, wavenumber and roll orientation to be found exactly. The asymptotic theory that permits these quantities to be determined requires Re and Ω to be small, in which case it is only their ratio (a Rossby number) that influences the orientation of the critical rolls. The numerical results confirm that this result remains valid for moderately large Re and Ω.

The limits of small and large Rossby number (in which rotation and shear, respectively, dominate) correspond to different values of the winding number $\mathscr{N}$. In the former limit, the critical rolls slavishly align with the rotation vector, and in the latter they remain roughly aligned with the shear regardless of the angle between the shear and the rotation vector. The integer nature of $2\mathscr{N}$ then implies at least one discontinuity of the winding number as the Rossby number is varied for fixed Ω or Re. Near such a discontinuity, the orientation of the critical rolls becomes a very sensitive function of the angle between the rotation vector and the shear flow when these are approximately at right angles. A slight change in this angle can cause the orientation of the critical rolls to change by almost a right angle.

The results we have described scratch the surface of the problem of convection in a rotating layer of fluid with an imposed shear flow. We could, for example, allow the shear flow to be driven not only by motion of the boundaries, but also by an imposed pressure gradient, to generate a range of Poiseuille–Couette flows (cf. Busse & Kropp 1992). These would have their own hydrodynamic instabilities that would influence the onset of motion. In general we should allow a vertical component of the rotation vector $\boldsymbol{\Omega}$. This complicates the basic-state shear flow, which is then no longer unidirectional (unless we introduce a fictitious force to keep it so) and is instead an Ekman spiral. Of course the complication is computational and not conceptual.

All the results we have described concern the case where instability sets in with the passage of a real eigenvalue through zero. For small Prandtl numbers, Kropp & Busse (1991) have shown that an oscillatory bifurcation occurs instead, which we have not analysed. Oscillatory convection in the form of travelling waves is also to be expected when the up–down symmetry is broken, for example by imposing different

boundary conditions at the top and bottom of the layer, or by using a cylindrical or spherical geometry.

Our emphasis has been on the linearized theory, but we have reported also on a small number of direct numerical simulations of the full three-dimensional nonlinear governing equations. These simulations show that while the linearized theory may predict the finite-amplitude solution well in some cases, many questions still remain about the interaction between different flow structures in the nonlinear regime.

We gratefully acknowledge financial support from the Nuffield Foundation (through Newly Appointed Science Lecturers awards to S.M.C. and P.C.M.), the University of Nottingham (through a New Lecturers Research Grant to S.M.C. and P.C.M.) and the Royal Society (P.C.M.).

REFERENCES

Acheson, D. J. 1990 *Elementary Fluid Dynamics*. Oxford University Press.

Auer, M., Busse, F. H. & Clever, R. M. 1995 Three-dimensional convection driven by centrifugal buoyancy. *J. Fluid Mech.* **301**, 371–382.

Busse, F. H. 1970 Über notwendige und hinreichende Kriterien für die Stabilität von Strömungen. *Z. Angew. Math. Mech.* **50**, 173–174.

Busse, F. H. 1982 Generation of mean flows in a rotating convection layer. *Z. Naturforsch.* **37a**, 752–758.

Busse, F. H. & Kropp, M. 1992 Buoyancy driven instabilities in rotating layers with parallel axis of rotation. *Z. Angew. Math. Phys.* **43**, 28–35.

Busse, F. H. & Riahi, N. 1980 Nonlinear convection in a layer with nearly insulating boundaries. *J. Fluid Mech.* **96**, 243–256.

Chandrasekhar, S. 1961 *Hydrodynamic and Hydromagnetic Stability*. Oxford University Press.

Chapman, C. J. & Proctor, M. R. E. 1980 Nonlinear Rayleigh-Bénard convection between poorly conducting boundaries. *J. Fluid Mech.* **101**, 759–782.

Clever, R. M. & Busse, F. H. 1992 Three-dimensional convection in a horizontal fluid layer subjected to a constant shear. *J. Fluid Mech.* **234**, 511–527.

Cox, S. M. 1996 The onset of thermal convection between poorly conducting horizontal boundaries in the presence of a shear flow. *SIAM J. Appl. Maths* **56**, 1317–1328.

Cox, S. M. 1997 Long-wavelength thermal convection in a weak shear flow. *IMA J. Appl. Maths* **58**, 159–184.

Cox, S. M., Leibovich, S., Moroz, I. M. & Tandon, A. 1992 Nonlinear dynamics in Langmuir circulations with O(2) symmetry. *J. Fluid Mech.* **241**, 669–704.

Cox, S. M. & Matthews, P. C. 1997 A pseudo-spectral code for convection with an analytical/numerical implementation of horizontal boundary conditions. *Intl J. Numer. Meth. Fluids.* **25**, 151–166.

Deardorff, J. W. 1965 Gravitational instability between horizontal plates with shear. *Phys. Fluids* **8**, 1027–1030.

Fujimura, K. & Kelly, R. E. 1988 Stability of unstably stratified shear flow between parallel plates. *Fluid Dyn. Res.* **2**, 281–292.

Fujimura, K. & Kelly, R. E. 1995 Interaction between longitudinal convection rolls and transverse waves in unstably stratified plane Poiseuille flow. *Phys. Fluids* **7**, 68–79.

Gallagher, A. P. & Mercer, A. McD. 1965 On the behaviour of small disturbances in plane Couette flow with a temperature gradient. *Proc. R. Soc. Lond.* A **286**, 117–128.

Gottlieb, D. & Orszag, S. A. 1977 *Numerical Analysis of Spectral Methods: Theory and Applications.* SIAM, Philadelphia.

Hathaway, D. H. & Somerville, R. C. 1986 Nonlinear interactions between convection, rotation and flows with vertical shear. *J. Fluid Mech.* **164**, 91–105.

Hathaway, D. H., Toomre, J. & Gilman, P. A. 1980 Convective instability when the temperature gradient and rotation vector are oblique to gravity. II. Real fluids with effects of diffusion. *Geophys. Astrophys. Fluid Dyn.* **15**, 7–37.

Ingersoll, A. P. 1966 Convective instabilities in plane Couette flow. *Phys. Fluids* **9**, 682–689.

Joseph, D. D. & Carmi, S. 1969 Stability of Poiseuille flow in pipes, annuli, and channels. *Q. Appl. Maths.* **26**, 575–599.

Kelly, R. E. 1994 The onset and development of thermal convection in fully developed shear flows. *Adv. Appl. Mech.* **31**, 35–112.

Kropp, M. & Busse, F. H. 1991 Thermal convection in differentially rotating systems. *Geophys. Astrophys. Fluid Dyn.* **61**, 127–148.

Mohamad, A. A. & Viskanta, R. 1989 Stability of lid-driven shallow cavity heated from below. *Intl J. Heat Mass Transfer* **32**, 2155–2166.

Pedley, T. J. 1969 On the instability of viscous flow in a rapidly rotating pipe. *J. Fluid Mech.* **35**, 97–115.

Proctor, M. R. E. 1981 Planform selection by finite-amplitude thermal convection between poorly conducting slabs. *J. Fluid Mech.* **113**, 469–485.

Winfree, A. T. 1980 *The Geometry of Biological Time*. Springer.